Compressive splitting failure of composites using modified shear lag theory

CHANDRA S. YERRAMALLI and ANTHONY M. WAAS*
Aerospace Engineering Department, University of Michigan, Ann Arbor, MI 48109-2140, U.S.A
(*Author for correspondence: Fax: 734 763 0578; E-mail: dcw@umich.edu)

Abstract. The shear lag model has been used in conjunction with the 3D elasticity equations to determine the stress state in a fiber/matrix system containing an interface crack. The use of a shear lag model to capture the stress state at the crack tip and the modelling of the region away from the crack tip by the elasticity equations leads to a simple analytical expression which can be used to determine the compliance changes for both unsteady crack growth as well as steady state crack propagation under compressive loading. Certain modifications to the assumptions used in the classical shear lag model have been made to increase the accuracy of the predictions for the rate of change of compliance with respect to crack length, dc/dl. The present approach leads to closed form expressions for the compressive strength of unidirectional fiber reinforced composites.

Key words: Compression, splitting, strain energy release rate, polymer matrix composites, shear lag

1. Introduction

It has long been recognised that the compressive strength of polymer matrix composites is the limiting factor for the use of composites in primary load hearing structures. The compression strength of polymer matrix composites is almost half of its tensile strength. Thus, understanding the behavior of polymer matrix composites under compression loading has been an active area of research. The interested reader is referred to the review paper by Waas and Schultheisz (1996) which provides an exhaustive coverage of the literature in this field. From the available literature it is clear that the composite compressive strength is found to be dependent on various parameters like fiber radius, fiber-matrix interfacial properties, misalignment of fibers, fiber packing density, fiber volume fraction and strain gradients. Research on developing models to predict the compressive strength of composites have focussed on including the above parameters in their formulation. (Drapier et al. (2001). Wisnom and Atkinson (1997) have studied the effect of strain gradients on compressive failure and found that the compressive strength increased under bending compression loading compared to pure compression loading. From the experimental investigations carried out by previous researchers (Kyriakides et al., 1995; Fleck, 1997; Lee, 1998; Lee and Waas, 1999; Oguni and Ravichandran, 2000) it can be inferred that the initiating mechanisms for compressive failure of composite materials are usually microbuckling and kinking of fibers aligned along the loading direction.

Lee (1998), Lee and Waas (1999) and Oguni and Ravichandran (2000) observed that glass fiber reinforced polymer matrix composites fail predominantly by splitting. This was observed in the optical photomicrographs which show aligned cracks between the fiber and matrix, indicating that splitting failure is akin to interfacial fiber/matrix fracture. Thus a fracture mechanics based approach was adopted by Lee (1998) and Lee and Waas (1999) to model

the splitting failure of polymer matrix composites. Their model was based on linear elastic fracture mechanics and the assumption of steady state crack propagation. Independently, Oguni and Ravichandran (2000) also provided fracture mechanics based expressions for the compression splitting failure stress of composites. These authors also examined the influence of confinement on compression strength. The stress analysis in Lee and Waas (1999) included areas in the cracked and uncracked regions of the composite and excluded a small region of size ϵ around the crack tip. In this region the stress state is a function of the crack tip field. When the crack is propagating under steady state conditions, this region translates with the crack tip. Thus, the rate of change of compliance with crack length is unaffected. The expression for the rate of change of compliance dc/dl is also independent of the crack length or the initial fiber length. For short cracks, where the crack propagation is unsteady, Lee and Waas (1999) used the finite element method to extract the dependency of dc/dl on crack length. A major goal of the present work is obtaining a closed form expression for the change in compliance dc/dl as a function of crack length. This expression can then be used in determining the compressive stress of a polymer matrix composite in terms of its fracture toughness γ_f and dc/dl in closed form. For this purpose a modified shear lag model has been used to study the stress state at the crack tip. The local shear lag based stress field has been superposed on the far field stress state of the composite obtained from the 3D elasticity equations, to obtain expressions for compliance and compliance change as a function of the crack length. In the development of this shear lag based model, only perfectly aligned fibers have been considered. The inclusion of misalignment will result in a change in the stiffness of the fiber and has already been treated in the steady-state splitting model by Lee and Waas (1999). The validation of the splitting model based on the steady state crack propagation assumption with experimental results presented in Lee and Waas (1999) indicates a good correlation.

2. Stress Analysis

Consider a representative volume element (RVE) of the composite containing a single fiber of length 2L with a crack of length 2l embedded in it as shown in Figure 1. The single fiber is divided into four regions for the purpose of deriving an expression for compliance and the rate of change of compliance. By symmetry, only one side of the fiber ($0 < z < L$), containing the crack region ($0 < z < l$) is modeled. Assume that a region ϵ extends from the crack tip in the positive Z axis direction as well as in the negative Z axis direction. The region extending beyond ϵ is modeled as in the case of the steady state splitting model as shown in Lee and Waas (1999).

2.1. SHEAR LAG ANALYSIS

The main assumptions in the traditional shear lag model of Cox (1952), are that the matrix carries only shear and any axial straining in the matrix is only for the purpose of load introduction. The fiber can only undergo axial contraction or extension and the fiber axial stress is zero at the fiber ends. It was observed by the authors that the classical shear lag method based on the above assumptions leads to a reasonably accurate calculation of the compliance of a cracked fiber/matrix system. But the rate of change of compliance with crack length, dc/dl turns out to be inaccurate. This in turn leads to the inaccurate calculation of strain energy release rate. In the present work the traditional shear lag parameter
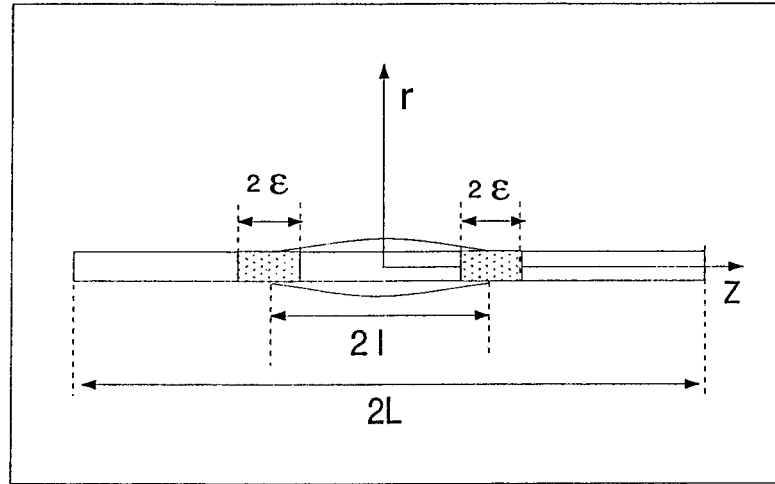
a)   A single fiber with a crack embedded in matrix
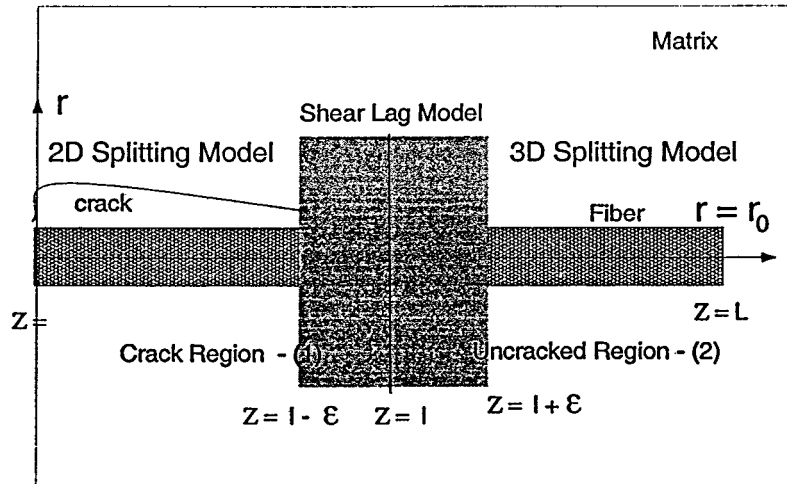
b) Crack and Uncracked regions

Figure 1. RVE showing the various regions of analysis.

$$\eta_{\text{cox}}^2 = \frac{1}{r_0^2} \frac{2E_m}{E_f(1 + v_m)\ln(1/V_f)}$$

as proposed by Cox (1952) has been used along with a modified set of boundary conditions since it gives an accurate value of the change in compliance with respect to crack length, dc/dl, in addition to preserving the accuracy of the compliance calculation.

For the present work, we assume that the fiber ends do carry some load and that the shear lag method is valid over the small region extending from $(l - \epsilon)$ to $(l + \epsilon)$. These modifications are introduced into the shear lag model by ensuring that the fiber axial stress at $z = (l + \epsilon)$, matches with the fiber axial stress of the uncracked region calculated using the 3D equations of elasticity. Also, at $z = (l - \epsilon)$, the fiber axial stress is equated with the steady state splitting
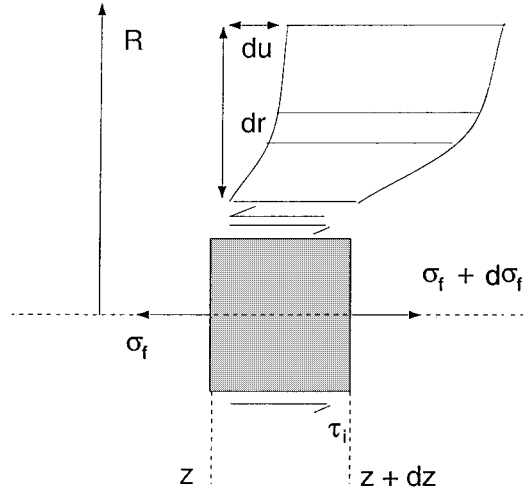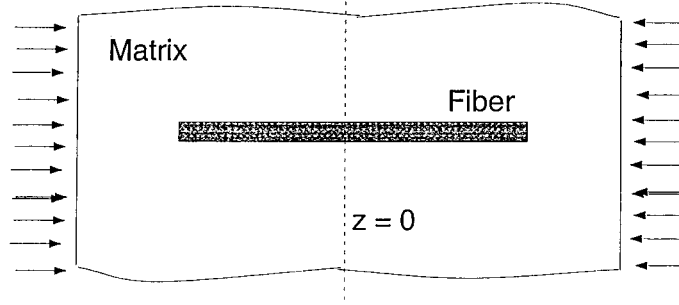
Classical shear lag model

Figure 2. Free body diagram of a small segment of fiber and attached matrix.

model stress in the crack region, which is similar to what is obtained via a simple rule of mixtures based stress prediction.

Taking a small segment dz of the composite containing the single fiber as shown in Figure 2, we can get the radial variation of shear stress in the matrix, $\hat{\tau}$ by equating the shear farces on neighboring annuli with radii r_1 and r_2 of length dz. Then,

$$2\pi r_1 \hat{\tau}_1 \, dz = 2\pi r_2 \hat{\tau}_2 \, dz.$$

From the above equation, we get the relation between $\hat{\tau}_1$ and $\hat{\tau}_2$ as $\hat{\tau}_1/\hat{\tau}_2 = r_2/r_1$. Thus at any radius r, we can relate the shear stress $\hat{\tau}(r)$ to the interface shear stress $\hat{\tau}_i$.

To obtain the relation between shear strain and shear stress, consider the displacement $\hat{u}_r(z)$ of the matrix with respect to the unstressed position. Then

$$\frac{d\hat{u}}{dr} = \gamma = \frac{\hat{\tau}_r}{G_m} = \frac{\hat{\tau}_i}{G_m}\left(\frac{r_0}{r}\right) \quad \text{or} \quad d\hat{u} = \frac{\hat{\tau}_i}{G_m}\left(\frac{r_0}{r}\right) dr.$$

Integrating the above equation between $r = r_0$ and $r = R$, we obtain

$$\int_{\hat{u}_r=(r_0)}^{\hat{u}_r=(R)} d\hat{u} = \frac{\hat{\tau}_i r_0}{G_m} \ln\left(\frac{R}{r_0}\right) = \hat{u}_R - \hat{u}_{r_0},$$

where $\hat{u}_R$ is the matrix displacement at a distance R from the fiber and $\hat{u}_{r_0}$ is the matrix displacement at interface $r = r_0$. The value of R is based on the assumption that the matrix strain is uniform, remote from the fiber-matrix interface. Thus the appropriate value of R is dictated by the proximity of fibers which in turn depends on the fiber packing and fiber volume fraction V_f. Assuming a hexagonal packing of fibers (Hashin and Rosen, 1964) and also taking note of the fact that the ratio R/r_0 appears as a logarithmic term and is relatively insensitive to the details of geometry, we can write the following expression relating fiber volume fraction V_f and the ratio R/r_0.

$$V_f = \frac{\pi r_0^2}{2\sqrt{3}R^2}, \qquad \left(\frac{R}{r_0}\right)^2 \approx \frac{1}{V_f}.$$

From Figure 2b, by equating the farces acting along the axial direction of the fiber we get the relation between the axial stress in the fiber and the interfacial shear stress.

$$2\pi r_0 \hat{\tau}_i \, dz = -\pi r_0^2 \, d\hat{\sigma} f, \qquad \frac{d\hat{\sigma}_f}{dz} = \frac{-2\hat{\tau}_i(z)}{r_0}.$$

Combining the above expression with the expression for interfacial shear stress $\hat{\tau}_i$ in terms of the displacements we get

$$\frac{d\hat{\sigma}_f}{dz} = \frac{-2E_m}{(1+\nu_m)\, r_0^2\, \ln(1/V_f)} \frac{(\hat{u}_R - \hat{u}_{r_0})}{}, \tag{1}$$

differentiating Equation (1), we get

$$\begin{aligned}\frac{d^2\hat{\sigma}_f}{dz^2} &= \frac{-2E_m}{(1+\nu_m)r_0^2\, \ln(1/V_f)} \left(\frac{d\hat{u}_R}{dz} - \frac{d\hat{u}_{r_0}}{dz}\right) \\ &= \frac{\eta^2}{r_0^2}(\hat{\sigma}_f - \hat{\epsilon}_m E_f)\end{aligned} \tag{2}$$

In the above expression the following substitutions have been made.

$$\left.\frac{d\hat{u}}{dz}\right|_{r=r_0} = \hat{\epsilon}_f = \frac{\hat{\sigma}_f}{E_f}, \quad \left.\frac{d\hat{u}}{dz}\right|_{r=R} = \hat{\epsilon}_m, \quad \eta^2 = \frac{2E_m}{E_f(1+\nu_m)\, \ln(1/V_f)},$$

where $\hat{\epsilon}_m$ is the matrix strain, $\hat{\epsilon}_f$ is the fiber axial strain, $\hat{\sigma}_f$ is the fiber stress and E_f is axial fiber modulus.

Equation (2) is a second order ordinary differential equation, whose solution is

$$\hat{\sigma}_f(z) = E_f\hat{\epsilon}_m + B\, \sinh\left(\frac{\eta z}{r_0}\right) + D\, \cosh\left(\frac{\eta z}{r_0}\right). \tag{3}$$

2.2. SPLITTING MODEL – SHEAR LAG METHOD

In this section we present the details of the application of the shear lag model to the splitting model analysis of Lee and Waas (1999). For this purpose, the RVE can be divided into two regions - the crack region and the uncracked region.

2.2.1. *Crack region*
In this region it is reasonable to assume that the fiber axial stress is equal to that of the axial stress obtained from the splitting model with increasing distance from the crack tip. Also in the crack region according to the shear lag model there is no shear stress hence the fiber axial stress is constant. Thus,

$$\frac{d\hat{\sigma}_{f(1)}}{dz} = 0,$$

$$\Rightarrow \hat{\sigma}_{f(1)} = A,$$

$$\Rightarrow \hat{\epsilon}_{f(1)} = \frac{A}{E_f}.$$

Integrating the expression for fiber axial strain we get $\hat{u}_{f(1)} = (A/E_f)z$ where the constant of integration has been taken to be zero since it represents a rigid body translation. The expressions for the stress and displacement field from the splitting model for the crack region are as given in Lee and Waas (1999).

$$\hat{\sigma}_{f2D} = \frac{PE_f}{\pi r_0^2 \delta},$$

from which we can obtain

$$\hat{u}_{f2D} = \frac{P}{\pi r_0^2 \delta} z,$$

where

$$\delta = E_f + E_m \left(\frac{1}{V_f} - 1 \right).$$

2.2.2. *Uncracked region*

In the uncracked region, we can take the expression of normal fiber stress as given by Equation (3). However in the present analysis this expression is valid in the region $l < z < l + \epsilon$. For $z > l + \epsilon$, the normal stress expression corresponding to the 3D equations of elasticity, is taken from the splitting model. Thus, at $z = l + \epsilon$, we equate the fiber normal stress $\hat{\sigma}_{f(2)}$ obtained from the shear lag analysis with that of the fiber normal stress obtained from the splitting model. Also, at the interface between the crack and uncracked region continuity of fiber normal stress and axial displacements is enforced. The expression for normal fiber strain can be obtained from Equation (3) and is as follows.

$$\hat{\epsilon}_{f(2)} = \hat{\epsilon}_m + \frac{B}{E_f} \sinh \left(\frac{\eta z}{r_0} \right) + \frac{D}{E_f} \cosh \left(\frac{\eta z}{r_0} \right).$$

On integrating the above, we get

$$\hat{u}_{f(2)} = \hat{\epsilon}_m z + \frac{B}{E_f} \frac{r_0}{\eta} \cosh \left(\frac{\eta z}{r_0} \right) + \frac{D}{E_f} \frac{r_0}{\eta} \sinh \left(\frac{\eta z}{r_0} \right) + C2.$$

Similarly an expression for the displacement field in the region beyond $z = l + \epsilon$ can be obtained from the 3D splitting model analysis and is as follows

$$u_{3d} = \frac{\beta P}{\pi r_0^2} z + C2$$

The expression for the stress σ_{3d} is as follows (Lee and Waas, 1999),

$$\sigma_{3d} = \frac{\beta P}{\pi r_0^2} (E_m - 4\alpha v_m (v_f - v_m)),$$

where

$$\alpha = \left[\frac{2(1+v_f)(1-2v_f)}{E_f}(V_f^{-1}-1) + \frac{2(1+v_m)(1-2v_m+V_f^{-1})}{E_m} \right]^{-1},$$

$$\beta = [E_f + (V_f^{-1}-1)\{E_m + 4\alpha(v_f - v_m)^2\}]^{-1}. \tag{4}$$

The following boundary conditions can be written for the present boundary value problem.
Crack region
at

$$z = l - \epsilon, \qquad \hat{\sigma}_{f(1)} = \sigma_{f2D}, \Rightarrow A = \frac{PE_f}{\pi r_0^2 \delta}$$

and hence

$$\hat{u}_{f(1)} = \frac{P}{\pi r_0^3 \delta}(l - \epsilon).$$

Further, at $z = l$

$$\hat{u}_{f(1)} = \hat{u}_{f(2)}.$$

From the condition for continuity of displacement across the crack interface the constant $C2$ is evaluated which is then used to get the displacement field $\hat{u}_{f(2)}$ to be,

$$\hat{u}_{f(2)} = \frac{P}{\pi r_0^2 \delta} + \frac{B}{E_f}\frac{r_0}{\eta}\left[\cosh\left(\frac{\eta z}{r_0}\right) - \cosh\left(\frac{\eta l}{r_0}\right)\right] + \frac{D}{E_f}\frac{r_0}{\eta}\left[\sinh\left(\frac{\eta z}{r_0}\right) - \sinh\left(\frac{\eta l}{r_0}\right)\right]. \tag{5}$$

At $z = l$, the continuity of normal stresses provides

$$\hat{\sigma}_{f(1)} = \hat{\sigma}_{f(2)}, \qquad \frac{PE_f}{\pi r_0^2 \delta} = E_f \hat{\epsilon}_m + B\,\sinh\left(\frac{\eta l}{r_0}\right) + D\,\cosh\left(\frac{\eta l}{r_0}\right). \tag{6}$$

Uncracked region

at $z = l + \epsilon$

$$\hat{\sigma}_{f(2)} = \sigma_{f3D},$$

which translates to

$$E_f \hat{\epsilon}_m + B\,\sinh\left(\frac{\eta(l+\epsilon)}{r_0}\right) + D\,\cosh\left(\frac{\eta(l-\epsilon)}{r_0}\right) = \frac{\beta P}{\pi r_0^2}[E_m - 4\alpha v(v_f - v_m)]. \tag{7}$$

To ensure compatibility, we equate the displacements $u_{f(2)}$ and u_{f3D}. This provides,

$$\hat{\epsilon}_m(l+\epsilon) + \frac{B}{E_f}\frac{r_0}{\eta}\cosh\left(\frac{\eta(l+\epsilon)}{r_0}\right) +$$

$$\frac{D}{E_f}\frac{r_0}{\eta}\sinh\left(\frac{\eta(l+\epsilon)}{r_0}\right) = \frac{\beta P(l+\epsilon)}{\pi r_0^2} + C3 \tag{8}$$

Equation (8) enables to obtain the constant $C3$ in terms of the remaining constants B and D. The constants B and D can be evaluated from the two Equations (6) and (7). Knowing B and D, $C3$ and $C2$ can be determined. Expressions for the constants B and D are given below.

$$D = \frac{\Theta}{\left[\dfrac{\cosh\left(\dfrac{\eta l}{r_0}\right) \sinh\left(\dfrac{\eta(l+\epsilon)}{r_0}\right)}{\sinh\left(\dfrac{\eta l}{r_0}\right)} - \cosh\left(\dfrac{\eta(l+\epsilon)}{r_0}\right) \right]},$$

$$B = \frac{-\cosh\left(\dfrac{\eta l}{r_0}\right)\Theta}{\sinh\left(\dfrac{\eta l}{r_0}\right) \left[\dfrac{\cosh\left(\dfrac{\eta l}{r_0}\right) \sinh\left(\dfrac{\eta(l+\epsilon)}{r_0}\right)}{\sinh\left(\dfrac{\eta l}{r_0}\right)} - \cosh\left(\dfrac{\eta(l+\epsilon)}{r_0}\right) \right]},$$

where

$$\Theta = \frac{P}{\pi r_0^2} \left[\frac{E_f}{\delta} - \beta \left[E_f + 4\alpha v_f (v_f - v_m)\left(\frac{1}{V_f} - 1 \right) \right] \right].$$

The total axial displacement can be written in terms of the integrals of the fiber axial strains as follows.

$$\Delta = \underbrace{2 \int_0^l \hat{\epsilon}_{f(1)} \, dz}_{\text{Crack region}(1)} + \overbrace{2 \int_l^{(l+\epsilon)} \hat{\epsilon}_{f(2)} \, dz + 2 \int_{(l+\epsilon)}^L \epsilon_{f3D} \, dz}^{\text{Uncracked region}(2)}.$$

On substituting the expressions for the axial strains in the above integrals results in,

$$\Delta = 2 \int_0^l \frac{P}{\pi r_0^2 \delta} \, dz + 2 \int_l^{(l+\epsilon)} \left[\hat{\epsilon}_m + \frac{B}{E_f} \sinh\left(\frac{\eta z}{r_0}\right) + \frac{D}{E_f} \cosh\left(\frac{\eta z}{r_0}\right) \right] dz + 2 \int_{l+\epsilon}^L \frac{\beta P}{\pi r_0^2} dz. \tag{9}$$

We can observe from the above equations for total displacement Δ that as $\epsilon \to 0$ (meaning the region ϵ around the crack tip vanishes), the second integral vanishes and also the third reduces to the same expression as given in Lee and Waas (1999) giving us the displacement expression obtained with steady state crack propagation assumption.

3. Strain energy release rate

The total potential energy Π of the RVE under consideration, when subjected to a compressive load, P is $U - W$, where U is the strain energy stored in the RVE and W is the work clone. The expression for strain energy release rate is

$$G = \frac{d\Pi}{dA},$$

where $A = 4\pi r_0 l$ is the crack surface area and r_0 is the fiber radius. The overall compliance of the RVE, c is defined as:

$$c = \frac{\Delta}{P},$$ (10)

where Δ is the axial compressive displacement of the composite and P is the external compressive load. The expression for Δ is substituted from Equation (9). For either case of load control or displacement control, the strain energy release rate can be written as

$$G = \frac{P^2}{8\pi r_0} \frac{dc}{dl}.$$

The fracture toughness γ_f is half of the value of G at the time of initiation of crack propagation.

$$G = 2\gamma_f.$$

The compressive stress σ_c can be related to the fracture toughness of the material γ_f by the following the expression

$$\sigma_c = \sqrt{\frac{16\gamma_f V_f^2}{\pi r_0^3 \left(\dfrac{dc}{dl}\right)}}.$$ (11)

4. Solution

The expression for Δ in the form of the integral given in Equation (9) is evaluated to get the displacement.

$$\begin{aligned}
\Delta = \; & 2\left\{\frac{Pl}{\pi r_0^2 \delta} + \frac{P\epsilon}{\pi r_0^2 \delta} + \left\{\frac{B}{E_f}\left[\cosh\left(\frac{(l+\epsilon)\eta}{r_0}\right) - \cosh\left(\frac{l\eta}{r_0}\right)\right]\right.\right. \\
& \left.\left. + \frac{D}{E_f}\left[\sinh\left(\frac{(l+\epsilon)\eta}{r_0}\right) \sinh\left(\frac{l\eta}{r_0}\right)\right]\right\}\frac{r_0}{\eta} + \frac{P\beta(L-l-\epsilon)}{\pi r_0^2}\right\}.
\end{aligned}$$ (12)

We get the relation for compliance c by dividing Equation (12) by the load term P. Thus,

$$\begin{aligned}
c = \; & 2\left\{\frac{l}{\pi r_0^2 \delta} + \frac{\epsilon}{\pi r_0^2 \delta} + \left\{\frac{B}{E_f}\left[\cosh\left(\frac{(l+\epsilon)\eta}{r_0}\right) - \cosh\left(\frac{l\eta}{r_0}\right)\right]\right.\right. \\
& \left.\left. + \frac{D}{E_f}\left[\sinh\left(\frac{(l+\epsilon)\eta}{r_0}\right) - \sinh\left(\frac{l\eta}{r_0}\right)\right]\right\}\frac{r_0}{\eta} + \frac{\beta(L-l-\epsilon)}{\pi r_0^2}\right\}.
\end{aligned}$$ (13)

Equation (13), is an expression for compliance of the system in terms of the crack length, l, and crack tip influence zone ϵ. The rate of change of compliance, dc/dl is obtained by differentiating Equation (13) with respect to the crack length, l.

$$\begin{aligned}
\frac{dc}{dl} = \; & \frac{2}{\pi r_0^2}\left[\frac{1}{\delta} - \beta\right] + \left[\frac{r_0}{\eta E_f}\left(\frac{dB}{dl} + D\right)\left(\cosh\left(\frac{(l+\epsilon)\eta}{r_0}\right) - \cosh\left(\frac{l\eta}{r_0}\right)\right.\right. \\
& \left.\left. + \left(\frac{dD}{dl} + B\right)\left(\sinh\left(\frac{(l+\epsilon)\eta}{r_0}\right) - \sinh\left(\frac{l\eta}{r_0}\right)\right)\right]\right].
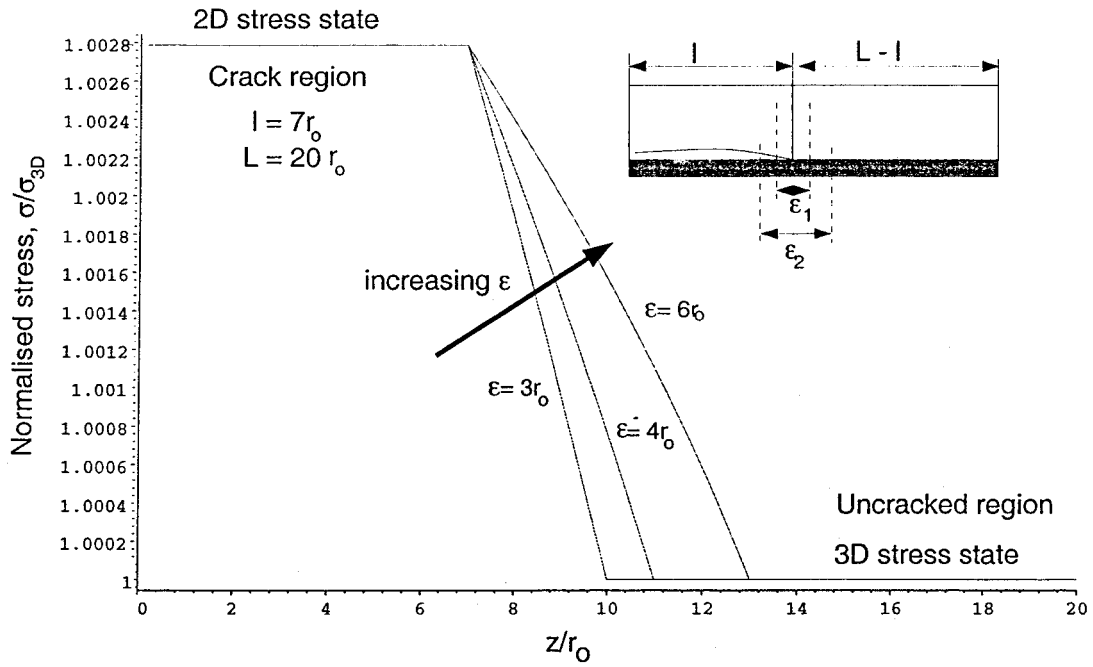\end{aligned}$$ (14)

Figure 3. Variation of normalised stress along the length of fiber as a function of increasing ϵ with crack length factor $n_1 = 7$.

It can be seen in the above equation that the first term corresponds to the steady state behavior (independent of crack length, l) and the second term, which contains the crack length l and the crack tip influence zone size ϵ, is due to non steady effects. The constants B and D in the above expression are functions of crack length l. For determining the rate of change of compliance with crack length, the previously described expressions were coded in MAPLE (symbolic math package) and evaluated for a glass/epoxy composite system of fiber volume fraction ($V_f = 10\%$). For the ease of calculation the half length of fiber L, half crack length l and the crack tip influence zone ϵ were all expressed as a factor of the fiber radius r_0. The fiber half length L was taken to be 20 times the the fiber radius for the present calculations. The normalized crack length $n_1 = l/r_0$, and the normalized crack tip zone, $n = \epsilon/r_0$, are used as parameters. Plots of normal stress variation along the length of fiber, compliance and rate of chance of compliance as a function of n_1 and n are shown in Figures 3–6. The following material properties of the glass fiber and vinyl-ester matrix were used in the analysis.

– Glass fiber

$$r_0 = 0.012 \text{ mm}, \qquad E_f = 72\,000 \text{ MPa}, \qquad \nu_f = 0.22.$$

– Vinyl-ester resin

$$E_m = 3585 \text{ MPa}, \qquad \nu_m = 0.36.$$

5. Discussion and conclusions

As the equation for the rate of change of compliance with crack length, dc/dl, indicates, compliance change is no longer independent of the crack length l or the crack tip influence zone
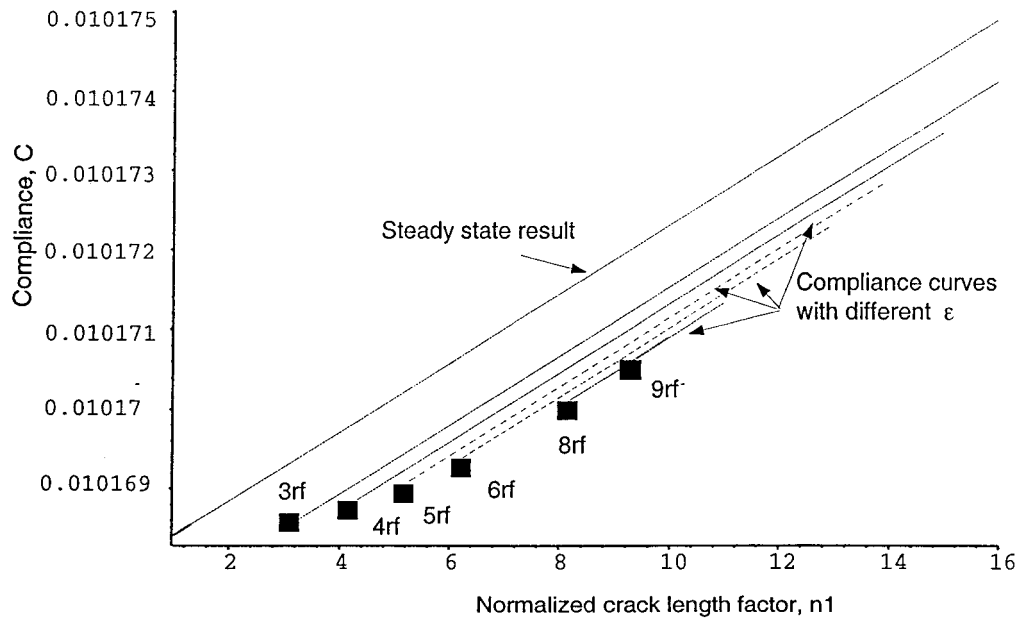
Figure 4. Curves of compliance as a function of normalized crack length for different values of ϵ and $L = 20r_0$.
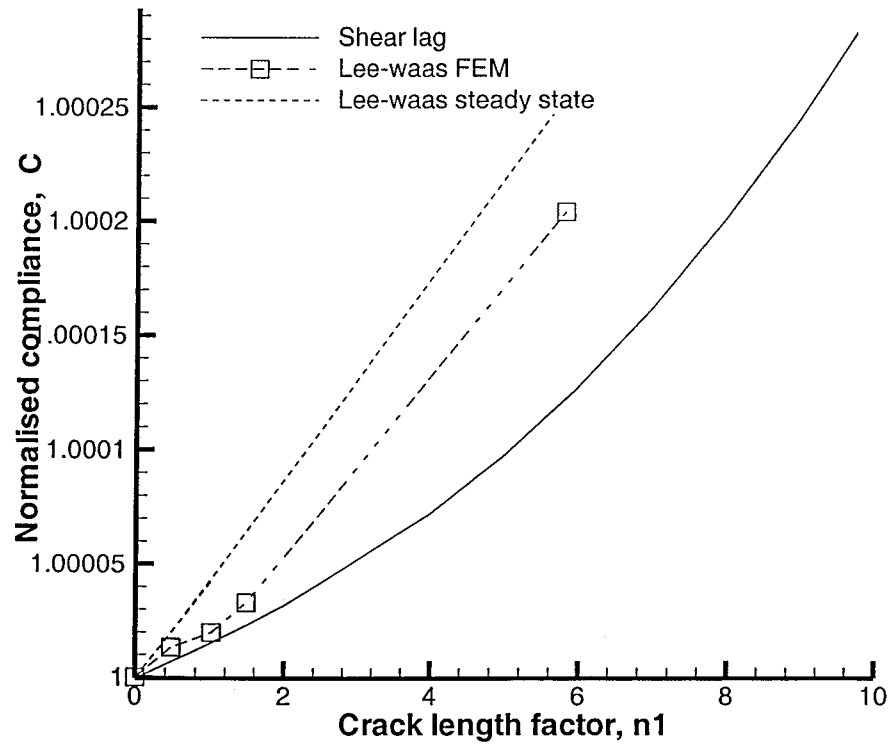

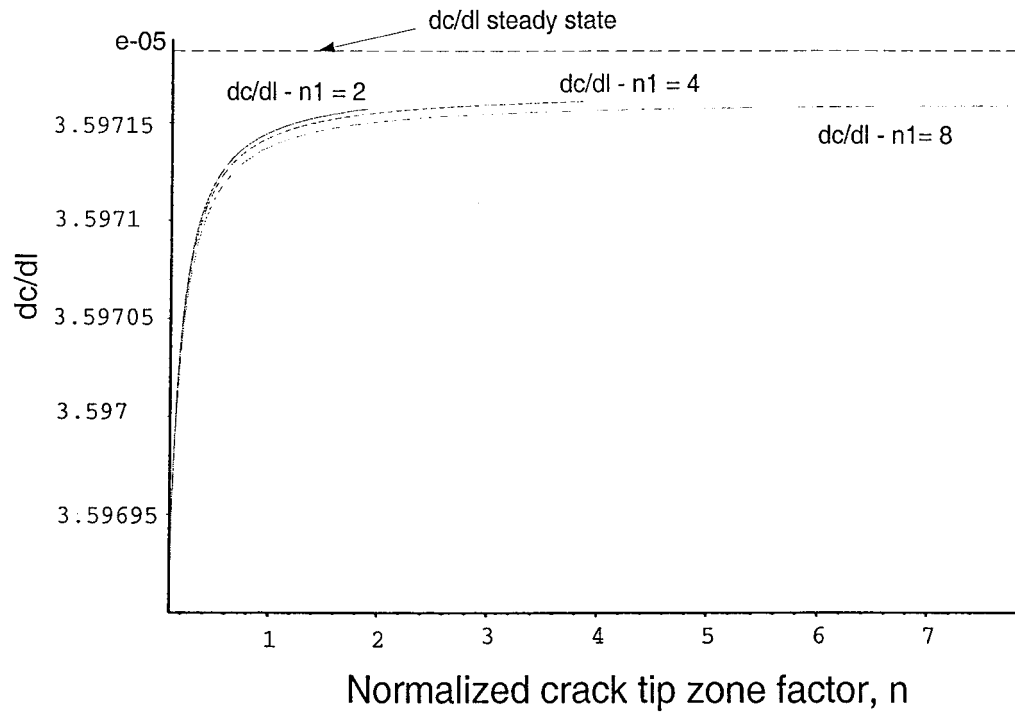*Figure 5.* Normalized compliance with normalized crack length factor, n_1.

Figure 6. Curves of rate of change of compliance with crack length dc/dl as a function of crack length with varying ϵ and $L = 20r_0$.

Table 1. dc/dl values obtained from splitting and FE models

	Glass/vinyl ester	
V_f	Splitting model dc/dl	FE model dc/dl
10	3.59715×10^{-5}	3.1881×10^{-5}
60	2.801×10^{-5}	2.4042×10^{-5}

Table 2. Compressive stress values obtained from splitting and FE models with $\gamma_f = 1.0546 \times 10^{-4}$ KJ m^{-2}

	Glass/vinyl ester	
V_f	Splitting model	FE model
10	298	312.25
60	1998.45	2157.36

parameter ϵ. However, the value of ϵ is initially unknown since the crack tip zone advances with the crack and also the region of influence does not remain constant. Thus the first step in evaluating dc/dl would be to determine the value of ϵ. However, before determining the value of ϵ, a study of the normal stress variation along the fiber length is necessary. A plot (Figure 3) of the normalised stress (σ_f/σ_{3D} with a normalised length factor (z/r_0) indicates that there is a discontinuity between the 2D stress state in the cracked region and the 3D stress state in the uncracked region, which is bridged by the modified shear lag model. The value of ϵ controls the gradient of the stress in this bridging region, with increasing values of ϵ decreasing the stress gradients. Hence, for a given crack length it is necessary to take ϵ as large as possible. But, it has to be kept in mind that the value of ϵ cannot exceed the half crack length l and at the same time ϵ should be smaller than $L - l$. As shown in Figure 4, the compliance of the fiber/matrix system is plotted as a function of the crack length parameter for different values of ϵ. For a particular ϵ we can see that the compliance vs crack length plots are straight lines, implying that the slope dc/dl is a constant. If we mark the lower tip of the straight lines with black dots as shown in Figure 4, we can observe that the slope of the locus of these points is initially varying and then approaches a constant af ter some crack length parameter n_1 indicating the steady state. The variation of compliance obtained from the present shear lag model, the FEM results (Lee and Waas, 1999), and the steady state expression are plotted as a function of crack length factor, n_1 and is shown in Figure 5. The slopes of all the three curves in the linear region are nearly equal. Similarly, for the compliance change dc/dl the curve of dc/dl vs ϵ as a function of n becomes nearly flat beyond $\epsilon \geq 1.5r_0$ as seen in Figure 6. It can be seen from Figure 6 that when the crack length is small, as expected dc/dl is a function of crack length and the crack tip zone, even if we take the crack tip zone, ϵ equal to the crack length, l.

The value of rate of change of compliance obtained with the present rated approach using the modified shear lag model is found to be 3.5971×10^{-5} (N/mm)$^{-1}$ which is approximately equal to the value obtained from the steady state analysis, 3.597186×10^{-5} (N/mm)$^{-1}$ and the FEM value of 3.1881×10^{-5} (N/mm)$^{-1}$ given in Lee and Waas (1999). This value of dc/dl was obtained for a ϵ of 0.024 mm and crack length, l of 0.096 mm. The total length of fiber considered was about $40r_0$. As seen in Figure 6, for this crack length and ϵ, the dc/dl value has reached its asymptotic value. Thus the present analysis incorporating the shear lag model to account for the crack tip stress state provides an analytical approach to study both unsteady crack growth of short cracks and steady state crack behavior as crack length increases. It replaces the need to resort to finite element based computation for short crack length (unsteady crack growth). In Tables 1 and 2, we have compared the compressive strength predictions of the splitting model using Equation (11) with the FEM data provided in Lee and Waas (1999) for fiber volume fractions of 10% and 60%. The value of fracture toughness for a perfectly aligned composites was taken from Lee and Waas (1999). It is seen that the predicted values of compressive splitting strength are very high for $V_f = 60\%$, indicating that splitting is not a failure mode. This was indeed observed during experiments where the specimens failed by a combination of kinking and splitting.

Acknowledgements

References

Cox, H.L. (1952). The elasticity and strength of paper on other fibrous materials. *British Journal Applied Physics* **3**, 72.

Drapier, S., Grandidier, J.-C. and Potier-Ferry, M. (2001). A structural approach of plastic microbuckling in long fibre composites: Comparison with theoretical and experimental results. *International Journal of Solids and Structures* **38**, 3877–3904.

Fleck, N.A. (1997). 'Compressive failure of fiber composites'. In: *Advances in applied mechanics*, Vol. 33. Academic Press, New York, pp. 43–117.

Hashin, Z. and Rosen, B.W. (1964). The elastic moduli of fiber reinforced materials. *Journal of Applied Mechanics*, Volume No. 31, 275–306.

Kyriakides, S., Arseculareatne, R., Perry, E.J. and Liechti, K.M. (1995). On the compressive failure of fiber reinforced composites. In: *Proceedings of the Sixtieth Birthday Celebration of Prof. W.G. Knauss. International Journal of Solids and Structures* **32**, 689–738.

Lee, S.H. (1998). Compressive behavior of fiber reinforced unidirectional composites, Ph.D. Thesis. Aeropsace Engineering Department, University of Michigan, Ann Arbor.

Lee, S.H. and Waas, A.M. (1999). Compressive response of fiber reinforced unidirectional composites. *International Journal of Fracture* **100**, 275–306.

Oguni, K. and Ravichandran, G. (2000). An energy-based model of longitudinal splitting in unidirectional fiber-reinforced composites. *Journal of Applied Mechanics* **67**, 437–443.

Waas, A.M. and Schultheisz, C.R. (1996). Compressive failure of composites parts I and II. *Progress in Aerospace Sciences* **32**, 1–78.

Wisnom, M.R. and Atkinson, J.W. (1997). Constrained buckling tests show increasing compressive strain to failure with increasing strain gradient. *Composites-Part A: Applied Science and Manufacturing* **28**, 959–964.